

ND-1195 291

MOMENT EXERTED ON A CONING PROJECTILE BY A SPINNING
LIQUID IN A CYLINDRIC. (U) ARMY BALLISTIC RESEARCH LAB
ABERDEEN PROVING GROUND MD G R COOPER JUN 88

27

UNCLASSIFIED

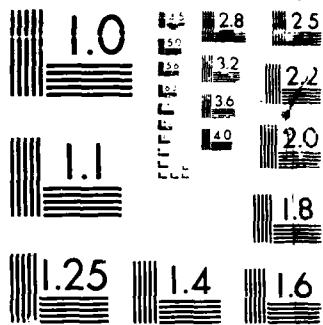
BRL-MR-3677

F/G 19/10

ML

002

1. *Chlorophyll a* (Chl *a*)
 2. *Chlorophyll b* (Chl *b*)
 3. *Chlorophyll c* (Chl *c*)
 4. *Chlorophyll d* (Chl *d*)
 5. *Chlorophyll e* (Chl *e*)
 6. *Chlorophyll f* (Chl *f*)
 7. *Chlorophyll g* (Chl *g*)
 8. *Chlorophyll h* (Chl *h*)
 9. *Chlorophyll i* (Chl *i*)
 10. *Chlorophyll j* (Chl *j*)
 11. *Chlorophyll k* (Chl *k*)
 12. *Chlorophyll l* (Chl *l*)
 13. *Chlorophyll m* (Chl *m*)
 14. *Chlorophyll n* (Chl *n*)
 15. *Chlorophyll o* (Chl *o*)
 16. *Chlorophyll p* (Chl *p*)
 17. *Chlorophyll q* (Chl *q*)
 18. *Chlorophyll r* (Chl *r*)
 19. *Chlorophyll s* (Chl *s*)
 20. *Chlorophyll t* (Chl *t*)
 21. *Chlorophyll u* (Chl *u*)
 22. *Chlorophyll v* (Chl *v*)
 23. *Chlorophyll w* (Chl *w*)
 24. *Chlorophyll x* (Chl *x*)
 25. *Chlorophyll y* (Chl *y*)
 26. *Chlorophyll z* (Chl *z*)
 27. *Chlorophyll aa* (Chl *aa*)
 28. *Chlorophyll ab* (Chl *ab*)
 29. *Chlorophyll ac* (Chl *ac*)
 30. *Chlorophyll ad* (Chl *ad*)
 31. *Chlorophyll ae* (Chl *ae*)
 32. *Chlorophyll af* (Chl *af*)
 33. *Chlorophyll ag* (Chl *ag*)
 34. *Chlorophyll ah* (Chl *ah*)
 35. *Chlorophyll ai* (Chl *ai*)
 36. *Chlorophyll aj* (Chl *aj*)
 37. *Chlorophyll ak* (Chl *ak*)
 38. *Chlorophyll al* (Chl *al*)
 39. *Chlorophyll am* (Chl *am*)
 40. *Chlorophyll an* (Chl *an*)
 41. *Chlorophyll ao* (Chl *ao*)
 42. *Chlorophyll ap* (Chl *ap*)
 43. *Chlorophyll aq* (Chl *aq*)
 44. *Chlorophyll ar* (Chl *ar*)
 45. *Chlorophyll as* (Chl *as*)
 46. *Chlorophyll at* (Chl *at*)
 47. *Chlorophyll au* (Chl *au*)
 48. *Chlorophyll av* (Chl *av*)
 49. *Chlorophyll aw* (Chl *aw*)
 50. *Chlorophyll ax* (Chl *ax*)
 51. *Chlorophyll ay* (Chl *ay*)
 52. *Chlorophyll az* (Chl *az*)
 53. *Chlorophyll aza* (Chl *aza*)
 54. *Chlorophyll abz* (Chl *abz*)
 55. *Chlorophyll acz* (Chl *acz*)
 56. *Chlorophyll adz* (Chl *adz*)
 57. *Chlorophyll aez* (Chl *aez*)
 58. *Chlorophyll afz* (Chl *afz*)
 59. *Chlorophyll agz* (Chl *agz*)
 60. *Chlorophyll ahz* (Chl *ahz*)
 61. *Chlorophyll aiz* (Chl *aiz*)
 62. *Chlorophyll ajz* (Chl *ajz*)
 63. *Chlorophyll akz* (Chl *akz*)
 64. *Chlorophyll alz* (Chl *alz*)
 65. *Chlorophyll amz* (Chl *amz*)
 66. *Chlorophyll anz* (Chl *anz*)
 67. *Chlorophyll aoz* (Chl *aoz*)
 68. *Chlorophyll apz* (Chl *apz*)
 69. *Chlorophyll aqz* (Chl *aqz*)
 70. *Chlorophyll arz* (Chl *arz*)
 71. *Chlorophyll asz* (Chl *asz*)
 72. *Chlorophyll atz* (Chl *atz*)
 73. *Chlorophyll auz* (Chl *auz*)
 74. *Chlorophyll avz* (Chl *avz*)
 75. *Chlorophyll awz* (Chl *awz*)
 76. *Chlorophyll axz* (Chl *axz*)
 77. *Chlorophyll ayz* (Chl *ayz*)
 78. *Chlorophyll azz* (Chl *azz*)
 79. *Chlorophyll azaa* (Chl *aza*
 80. *Chlorophyll abz* (Chl *abz*)
 81. *Chlorophyll acz* (Chl *acz*)
 82. *Chlorophyll adz* (Chl *adz*)
 83. *Chlorophyll aez* (Chl *aez*)
 84. *Chlorophyll afz* (Chl *afz*)
 85. *Chlorophyll agz* (Chl *agz*)
 86. *Chlorophyll ahz* (Chl *ahz*)
 87. *Chlorophyll aiz* (Chl *aiz*)
 88. *Chlorophyll ajz* (Chl *ajz*)
 89. *Chlorophyll akz* (Chl *akz*)
 90. *Chlorophyll alz* (Chl *alz*)
 91. *Chlorophyll amz* (Chl *amz*)
 92. *Chlorophyll anz* (Chl *anz*)
 93. *Chlorophyll aoz* (Chl *aoz*)
 94. *Chlorophyll apz* (Chl *apz*)
 95. *Chlorophyll aqz* (Chl *aqz*)
 96. *Chlorophyll arz* (Chl *arz*)
 97. *Chlorophyll asz* (Chl *asz*)
 98. *Chlorophyll atz* (Chl *atz*)
 99. *Chlorophyll auz* (Chl *auz*)
 100. *Chlorophyll avz* (Chl *avz*)
 101. *Chlorophyll awz* (Chl *awz*)
 102. *Chlorophyll axz* (Chl *axz*)
 103. *Chlorophyll ayz* (Chl *ayz*)
 104. *Chlorophyll azz* (Chl *azz*)
 105. *Chlorophyll azaa* (Chl *aza*
 106. *Chlorophyll abz* (Chl *abz*)
 107. *Chlorophyll acz* (Chl *acz*)
 108. *Chlorophyll adz* (Chl *adz*)
 109. *Chlorophyll aez* (Chl *aez*)
 110. *Chlorophyll afz* (Chl *afz*)
 111. *Chlorophyll agz* (Chl *agz*)
 112. *Chlorophyll ahz* (Chl *ahz*)
 113. *Chlorophyll aiz* (Chl *aiz*)
 114. *Chlorophyll ajz* (Chl *ajz*)
 115. *Chlorophyll akz* (Chl *akz*)
 116. *Chlorophyll alz* (Chl *alz*)
 117. *Chlorophyll amz* (Chl *amz*)
 118. *Chlorophyll anz* (Chl *anz*)
 119. *Chlorophyll aoz* (Chl *aoz*)
 120. *Chlorophyll apz* (Chl *apz*)
 121. *Chlorophyll aqz* (Chl *aqz*)
 122. *Chlorophyll arz* (Chl *arz*)
 123. *Chlorophyll asz* (Chl *asz*)
 124. *Chlorophyll atz* (Chl *atz*)
 125. *Chlorophyll auz* (Chl *auz*)
 126. *Chlorophyll avz* (Chl *avz*)
 127. *Chlorophyll awz* (Chl *awz*)
 128. *Chlorophyll axz* (Chl *axz*)
 129. *Chlorophyll ayz* (Chl *ayz*)
 130. *Chlorophyll azz* (Chl *azz*)
 131. *Chlorophyll azaa* (Chl *aza*
 132. *Chlorophyll abz* (Chl *abz*)
 133. *Chlor*



MICROCOPY RESOLUTION TEST CHART
NATIONAL BUREAU OF STANDARDS 1963-A

(4)

MEMORANDUM REPORT BRL-MR-3677

AD-A195 291

BRL

1938 - Serving the Army for Fifty Years - 1988

**MOMENT EXERTED ON A CONING PROJECTILE
BY A SPINNING LIQUID IN A CYLINDRICAL
CAVITY CONTAINING A POROUS MEDIUM**

GENE R. COOPER

DTIC
ELECTE
S JUL 07 1988 **D**
Chap D

JUNE 1988

APPROVED FOR PUBLIC RELEASE; DISTRIBUTION UNLIMITED.

U.S. ARMY LABORATORY COMMAND

**BALLISTIC RESEARCH LABORATORY
ABERDEEN PROVING GROUND, MARYLAND**

UNCLASSIFIED

SECURITY CLASSIFICATION OF THIS PAGE

REPORT DOCUMENTATION PAGE				Form Approved OMB No. 0704-0188	
1a. REPORT SECURITY CLASSIFICATION UNCLASSIFIED			1b. RESTRICTIVE MARKINGS		
2a. SECURITY CLASSIFICATION AUTHORITY			3. DISTRIBUTION / AVAILABILITY OF REPORT Approved for public release; distribution is unlimited.		
2b. DECLASSIFICATION / DOWNGRADING SCHEDULE					
4. PERFORMING ORGANIZATION REPORT NUMBER(S) BRL-MR-3677			5. MONITORING ORGANIZATION REPORT NUMBER(S)		
6a. NAME OF PERFORMING ORGANIZATION U.S. Army Ballistic Research Laboratory		6b. OFFICE SYMBOL (If applicable) SLCBR-LF	7a. NAME OF MONITORING ORGANIZATION		
6c. ADDRESS (City, State, and ZIP Code) Aberdeen Proving Ground, MD 21005-5066			7b. ADDRESS (City, State, and ZIP Code)		
8a. NAME OF FUNDING / SPONSORING ORGANIZATION U.S. Army Ballistic Research Laboratory		8b. OFFICE SYMBOL (If applicable) SLCBR-DD-T	9. PROCUREMENT INSTRUMENT IDENTIFICATION NUMBER		
8c. ADDRESS (City, State, and ZIP Code) Aberdeen Proving Ground, MD 21005-5066			10. SOURCE OF FUNDING NUMBERS		
PROGRAM ELEMENT NO. 62618A		PROJECT NO. 1L1 62618AH80	TASK NO.	WORK UNIT ACCESSION NO.	
11. TITLE (Include Security Classification) Moment Exerted on a Coning Projectile by a Spinning Liquid in a Cylindrical Cavity Containing a Porous Medium (U)					
12. PERSONAL AUTHOR(S) Cooper, Gene R.					
13a. TYPE OF REPORT Memorandum Report		13b. TIME COVERED FROM _____ TO _____	14. DATE OF REPORT (Year, Month, Day) 1988 April		15. PAGE COUNT 29
16. SUPPLEMENTARY NOTATION					
17. COSATI CODES			18. SUBJECT TERMS (Continue on reverse if necessary and identify by block number)		
FIELD	GROUP	SUB-GROUP	Cylindrical Cavity Inviscid Porous Media Rotating Liquid		
01	01				
19. ABSTRACT (Continue on reverse if necessary and identify by block number) White phosphorous (WP) impregnated felt wedges are used as a payload in the M825 improved smoke projectile. An assumption made in this work is that the WP is in a liquid state (i.e., temperature > 44 degrees C) where such payloads have been seen to cause flight instabilities. The analytical results given here formulate an initial effort to gain an understanding of the dynamics of a projectile interacting with a WP/felt payload. The analytical methods used here are a simple extension of previous methods used to describe bulk-filled liquid payloads. Moments are predicted due to an inviscid liquid moving through a ridged porous medium which is confined to a spinning cylindrical cavity undergoing coning motion. A drag term is added to the classical Stewartson theory which is used to describe the flow in the porous media. The cylindrical cavity is assumed to consist of several chambers of circular cross section and uniform height, each separated by solid endcaps. This porous media theory is used to calculate the total liquid side moments exerted by all the chambers in the cylinder. Results are presented for a range of coning frequencies, fineness ratios, and porous drag coefficients.					
20. DISTRIBUTION / AVAILABILITY OF ABSTRACT <input type="checkbox"/> UNCLASSIFIED/UNLIMITED <input checked="" type="checkbox"/> SAME AS RPT. <input type="checkbox"/> DTIC USERS			21. ABSTRACT SECURITY CLASSIFICATION UNCLASSIFIED		
22a. NAME OF RESPONSIBLE INDIVIDUAL Dr. Gene R. Cooper			22b. TELEPHONE (Include Area Code) (301)-278-2057		22c. OFFICE SYMBOL SLCBR-LF-A

ACKNOWLEDGMENTS

The author is deeply indebted to Dr. William P. D'Amico for suggesting this study. Dr. D'Amico spent many hours discussing the topics of this report with the author, as well as, editing the manuscript. The author also wishes to acknowledge the many helpful comments and suggestions received from Dr. Charles H. Murphy.



Accession For	
NTIS CRA&I	<input checked="" type="checkbox"/>
DTIC TAB	<input type="checkbox"/>
Unannounced	<input type="checkbox"/>
Justification	
By	
Distribution/	
Availability Codes	
Dist	Avail and/or Special
A-1	

TABLE OF CONTENTS

	<u>Page</u>
ACKNOWLEDGMENTS.....	iii
LIST OF FIGURES.....	vii
I. INTRODUCTION.....	1
II. LIQUID MOMENT.....	2
III. EQUATIONS OF LIQUID MOTION IN POROUS MEDIA.....	2
IV. LIQUID MOMENT EQUATIONS.....	6
V. NUMERICAL METHOD.....	8
VI. DISCUSSION.....	8
VII. CONCLUSIONS.....	10
REFERENCES.....	21
LIST OF SYMBOLS.....	23
DISTRIBUTION LIST.....	25

LIST OF FIGURES

<u>Figure</u>		<u>Page</u>
1	Diagram showing a typical cylindrical segment with impenetrable endcaps.....	11
2	C_{LSM} versus τ for $f = 1.5$, $C_r = 3$, $\epsilon = 0.0, 0.02$	12
3	C_{LIM} versus τ for $f = 1.5$, $C_r = 3$, $\epsilon = 0.0, 0.02$	13
4	Comparison of C_{LSM} versus τ for $f = 2$, $N = 1$, $\epsilon = 0$, $C_r = 3, 1, 0.5$	14
5	Comparison of C_{LIM} versus τ for $f = 2$, $N = 1$, $\epsilon = 0$, $C_r = 3, 1, 0.5$	15
6	Comparison of C_{LSM} versus τ for $f = 3$, $C_r = 3$, $\epsilon = 0$, $N = 1, 5, 10$ and C_{LSM} frozen.....	16
7	Comparison of C_{LIM} versus τ for $f = 3$, $C_r = 3$, $\epsilon = 0$, $N = 1, 5, 10$ and C_{LIM} frozen.....	17
8	Comparison of C_{LSM} versus τ for $f = 10$, $C_p = 3$, $\epsilon = 0.0$, $N = 1, 5, 10$	18
9	M825 improved smoke projectile.....	19

I. INTRODUCTION

Predicting the moment exerted by a liquid payload in a spinning and coning projectile is a problem of considerable interest to the Army. Stewartson¹ considered the linear problem of calculating the payload moment through the use of separation of variables and eigenvalue expansions for an inviscid liquid in a cylindrical cavity. First order viscous boundary layer corrections to the Stewartson theory were carried out by Wedemeyer² and Murphy.³ A method for calculating the linear liquid moment using the full viscous equations with boundary layer corrections confined only to the endcaps was also presented by Gerber and Sedney.⁴ They have recently extended this theory to eliminate the boundary layer correction at the endcaps.⁵

Liquid payloads contained in a highly permeable material have also been of interest to the Army for some time. Laboratory tests and flight tests have shown that a highly permeable medium can significantly reduce the spin-up time of a liquid payload.⁶ Flight stability for liquid saturated permeable payloads has also been examined by D'Amico.⁷

This report extends the Stewartson problem by considering a cylindrical cavity filled with a permeable medium that is impregnated with an inviscid liquid. A further modification is introduced by segmenting the cavity, along the symmetry axis, into a sequence of equal length cylinders. Each of these cylinders is separated by impermeable endcaps. The porous media is modeled by a drag term, which is proportional to the velocity field, added to the linearized Euler equations. This analysis examines the induced liquid moment as a function of parameters found by Stewartson plus parameters describing the porous media and the number of segments in the cylindrical cavity.

The nomenclature in this report is the same as that used by Murphy.³ In particular, this means that the liquid moment can be represented as the complex quantity:

$$\text{Transverse Moment} = m_L a^2 \dot{\phi}^2 \tau [C_{LSM} + i C_{LIM}] K_C e^{i\phi_C} \quad (1.1)$$

where

m_L is the mass of liquid in a fully-filled cavity,

a is the maximum radius of the container,

$\dot{\phi}$ is the inertial spin rate of the container along the symmetry axes,

τ is the ratio of coning rate to spin $\dot{\phi}_C/\dot{\phi}$,

C_{LSM} is the liquid side moment coefficient,

C_{LIM} is the liquid in-plane moment coefficient,

K_C is $\sin \alpha_C$ is the precession angle.

II. LIQUID MOMENT

Two coordinate systems, each with X-axis along the projectile symmetry axis, are used: the missile-fixed (X, Y, Z) system and the non-rolling $X\tilde{Y}\tilde{Z}$ system with the \tilde{Z} -axis initially pointing downward. Introduce an earth-fixed axes (X_e, Y_e, Z_e) with X_e -axis in the direction of the velocity vector and Z_e downward. Let a unit vector in the direction of the X-axis have earth-fixed components (n_{XE}, n_{YE}, n_{ZE}). The angle of attack $\tilde{\alpha}$ in the (X, \tilde{Y} , \tilde{Z}) system is the projection on the $X\tilde{Z}$ -plane of the angle between the X-axis and the velocity vector. The angle of sideslip $\tilde{\beta}$ is the projection of the same angle onto the $X\tilde{Y}$ -plane.

The kinematic behavior of the spinning projectile is the sum of two coning motions:³

$$\tilde{\xi} = \tilde{\beta} + i \tilde{\alpha} = K_1 e^{i\phi_1} + K_2 e^{i\phi_2} \quad (2.1)$$

where

$$\ln(K_j/K_{j0}) = \epsilon_j \tau_j \phi$$

$$\phi_j = \phi_{j0} + \tau_j \phi$$

$$\phi = \dot{\phi} t$$

($\dot{\phi} \geq 0$) is the spin rate and K_{j0}, ϕ_{j0} are constants.

III. EQUATIONS OF LIQUID MOTION IN POROUS MEDIA

The following analysis models the steady state response of a liquid flowing in a porous medium confined to a cylindrical cavity contained in a spinning and coning projectile. The objective of this theory is to predict the liquid moment resulting from coning or spiral motion which is specified by:³

$$\tilde{\xi} = \hat{K} e^{s\phi} \quad (3.1)$$

where

$$\hat{K} = K_{j0} e^{i\phi_{j0}}, \quad j = 1 \text{ or } 2$$

$$s = (\epsilon_j + i)\tau_j$$

The conservation equations governing the motion of the confined liquid are the continuity equation and a modified Euler-momentum equation. The modification is one that is commonly used to describe the flow of liquid through a porous medium. This consists of an additional term given by:

$$\vec{D}_r = -\frac{\mu}{\kappa} (\vec{V}_R) = -\rho_L a \dot{\phi}^2 C_r \left(\frac{\vec{V}_R}{a \dot{\phi}} \right) \quad (3.2)$$

where

μ is the dynamic viscosity

κ is the porosity (dimensions of length²)

\vec{V}_R is the velocity of liquid relative to the porous medium

ρ_L is liquid density

\vec{D}_r is a pressure gradient induced by resistance of the porous media to fluid flow.⁸ $C_r = \frac{\mu}{\rho_L K \dot{\phi}}$ is a

dimensionless coefficient which is a measure of this pressure gradient.

Physical reasons for using such equations can be found from the arguments used in establishing Darcy's Law.⁹

Let (r, θ, x) be cylindrical polar coordinates fixed to the earth frame and (V, W, U) be the corresponding components of velocity. For small angles, the position vector of any point in the projectile has components³

$$r = \tilde{r} - K_j \tilde{x} \cos(\phi_j - \tilde{\theta}) \quad (3.3)$$

$$x = \tilde{x} + K_j \tilde{r} \cos(\phi_j - \tilde{\theta}) \quad (3.4)$$

$$\theta = \tilde{\theta} + O(K_j^2) \quad (3.5)$$

where tilde (\sim) quantities are measured in the non-rolling system. Equations (3.3 - 3.5) lead to the velocity components

$$V_x = R \{ \dot{\phi} (s - i) r K e^{s\phi - i\theta} \} \quad (3.6)$$

$$V_r = -R \{ \dot{\phi} (s - i) x K e^{s\phi - i\theta} \} \quad (3.7)$$

$$V_\theta = \dot{\phi} r + R\{i\dot{\phi}(s-i)x\hat{K} e^{s\phi - i\theta}\} \quad (3.8)$$

where

$$R\{\} = [\{\} + \overline{\{\}}]/2 = \text{Real part of } \{\}.$$

Let the velocity, \vec{V} , and pressure, p , fields have the form:

$$\begin{aligned} \vec{V} &= \vec{q} + \dot{\phi} \hat{e}_x \times \vec{r} \\ P &= p + \frac{\rho_L \dot{\phi}^2 r^2}{2} \end{aligned} \quad (3.9)$$

where $\hat{e}_r, \hat{e}_\theta, \hat{e}_x$ are the unit vectors in the (r, θ, x) directions. The variables $\vec{q} = (v, w, u)$, and p are small perturbations of $O(K_j)$.

Non-dimensionalizing all lengths by the cylinder radius a and velocities by $a\dot{\phi}$, plus assuming periodic disturbances of the form

$$(v, w, u, p) = (v(r, x), w(r, x), u(r, x)) e^{s\phi - i\theta} \quad (3.10)$$

allows the continuity and momentum equations to be written as

$$\frac{\partial v}{\partial r} + \frac{v}{r} - \frac{iw}{r} + r \frac{\partial u}{\partial x} = 0 \quad (3.11)$$

$$(s-i)\vec{q} + 2\hat{e}_x \times \vec{q} = -\nabla p - C_r[\vec{q} + (s-i)(x, -ix, -r)]. \quad (3.12)$$

The components of Eq. (3.12) take the form

$$\gamma v - 2w + \frac{\partial p}{\partial r} = -(s-i) \times C_r \quad (3.13)$$

$$\gamma w + 2v - \frac{i p}{r} = i(s-i) \times C_r \quad (3.14)$$

$$\gamma u + \frac{\partial p}{\partial x} = (s-i) r C_r \quad (3.15)$$

where $0 \leq r \leq 1$, $h + f \leq x \leq h - f$

f = fineness ratio

$$\gamma = s - i + C_r$$

and h is the center of mass location along the symmetry axis. The non-homogeneous terms of Equations (3.13 - 3.15) suggest using the transformations

$$v = v_H - \frac{(s-i) \times C_r}{(\gamma + 2i)} \quad (3.16)$$

$$w = w_H + \frac{i (s-i) \times C_r}{(\gamma + 2i)} \quad (3.17)$$

$$u = u_H + \frac{(s-i) r C_r}{\gamma} \quad (3.18)$$

in the equations of motion which reduces them to a single equation for the pressure p

$$\frac{\partial^2 p}{\partial r^2} + \frac{1}{r} \frac{\partial p}{\partial r} - \frac{p}{r^2} = - \frac{(\gamma^2 + 4)}{\gamma^2} \frac{\partial^2 p}{\partial x^2} \quad (3.19)$$

Similarly, the solution p is related to the following physical quantities of interest:

$$v_H = \frac{1}{\gamma^2 + 4} \left[\frac{2ip}{r} - \gamma \frac{\partial p}{\partial r} \right] \quad (3.20)$$

$$w_H = \frac{1}{\gamma^2 + 4} \left[\frac{i\gamma p}{r} + 2 \frac{\partial p}{\partial r} \right] \quad (3.21)$$

$$u_H = - \frac{1}{\gamma} \frac{\partial p}{\partial x} \quad (3.22)$$

The cylindrical cavity is assumed to consist of N chambers with circular cross section and height $\Delta = 2f/N$, each separated by impenetrable endcaps as depicted in Figure 1.

The boundary conditions for Eq. (3.19) are the normal velocity of the fluid at the boundary must equal the normal velocity of the wall and all flow variables remain finite. This means:

$$\frac{\partial \hat{p}}{\partial x} = 0 \quad \text{at } x = h - f + n \left(\frac{2f}{N} \right) \quad (3.23)$$

$$n = 0, 1, \dots, N$$

$$2i\hat{p} - \gamma \frac{\partial \hat{p}}{\partial r} = -2xs(s-i)(s-3i+C_r) \quad \text{at } r = 1 \quad (3.24)$$

$$\hat{p} = 0 \quad \text{at } r = 0 \quad (3.25)$$

where $\hat{p} = p + xr(s-i)^2$. (3.26)

This boundary value problem is similar to the problem considered by Stewartson¹ and can be shown to have the solution

$$p = -xr(s-i)^2 + xs(s-i)[2(h-f) + (2n+1)\Delta]r +$$

$$\frac{16fs(s-i)(\gamma-2i)}{\pi^2 N} \sum_{k=\text{odd}}^{\infty} \frac{J_1(\lambda_k r) \cos \frac{\pi k}{\Delta} (x-h+f-n\Delta)}{k^2 [(2i+\gamma) J_1(\lambda_k) - \gamma \lambda_k J_0(\lambda_k)]} \quad (3.27)$$

where $\lambda_k^2 = -\frac{(\gamma^2+4)N^2 k^2 \pi^2}{\gamma^2 4 f^2}$; $N = 1, 2, 3, \dots$

$$n = 0, 1, \dots, N$$

and the J_n are the Bessel functions of the first kind. If γ is pure imaginary, the transcendental denominator in Eq. (3.27) will have zeroes. This resonant condition occurs whenever $\tau \epsilon + C_r = 0$ and τ is one of the inviscid Stewartson¹ eigenfrequencies.

IV. LIQUID MOMENT EQUATIONS

The moment induced by the liquid contained in the segmented cavity is calculated from the time derivative of the angular momentum field. Non-dimensionalizing this moment with $2\pi a^3 f \rho_L$ allows the moment in the YX plane to be expressed as a single complex quantity³

$$M_Y + i M_Z = \tau C_{LM} \hat{K} e^{s\phi} \quad (4.1)$$

where $C_{LM} = C_{LSM}(\tau, \epsilon, C_r, f) + i C_{LIM}(\tau, \epsilon, C_r, f).$

The unit vectors for the earth-fixed cylindrical coordinates, $(\hat{e}_r, \hat{e}_\theta, \hat{e}_x)$, can be written in the same complex notations in terms of $(\hat{e}_y, \hat{e}_z, \hat{e}_x)$

$$\hat{e}_r = \hat{e}_y \cos \theta + \hat{e}_z \sin \theta \Leftrightarrow e^{i\theta} \quad (4.2)$$

$$\hat{e}_\theta = -\hat{e}_y \sin \theta + \hat{e}_z \cos \theta \Leftrightarrow ie^{i\theta}. \quad (4.3)$$

Substituting these into the moment integral and using the Reynolds Transport Theorem¹⁰ gives the following expression for the liquid moment coefficient:

$$\tilde{\tau} C_{LM} = \frac{1}{2f} \sum_{n=0}^{N1-} \int_{h-f+n\Delta}^{h-f+(n+1)\Delta} \int_0^1 \{ (\tilde{x}\hat{e}_x + \tilde{r}\hat{e}_r) \times [(s-i)\vec{q} + 2\hat{e}_x \times \vec{q}] - i[\tilde{r}^2 - 2\tilde{x}^2] \} \tilde{r} d\tilde{r} d\tilde{x}. \quad (4.4)$$

Using Eqs. (3.16-3.18 and 3.20-3.22) with the aid of Eq. (3.27) permits writing the last equation as

$$\begin{aligned} \tilde{\tau} C_{LM} = & \frac{i}{12} \left[\frac{4[1-C_r(s-i)] [(s^2+1)(3h^2+f^2)] C_r}{(\gamma+2i)} + \frac{3[1+C_r(s-i)](s-i)^2 C_r}{\gamma} - \right. \\ & \left. 12h^2 - 4f^2 + 3 \right] + \frac{2is}{(\gamma+2i)} \left[\frac{(s^2+1)(3h^2+f^2)}{3} - \frac{2s(s-i)f^2}{N^2} \right] - \\ & \frac{128 i (s-i) (\gamma-2i) s^2 f^2}{(\gamma+2i) N^4 \pi^4} \sum_{k=\text{odd}}^{\infty} \frac{J_1(\lambda_k)}{k^4 [(\gamma+2i) J_1(\lambda_k) - \gamma \lambda_k J_0(\lambda_k)]}; \end{aligned} \quad (4.5)$$

$$N = 1, 2, 3, \dots$$

Murphy³ derived the frozen liquid values of C_{LSM} and C_{LIM} and these are given by

$$C_{LSM} = \frac{\epsilon}{2} \left[1 - \tau \left[1 + \frac{4(3h^2 + f^2)}{3} \right] \right] \quad (4.6)$$

$$C_{LIM} = \frac{1}{2} + \frac{\tau(\epsilon^2 - 1)}{12} [3 + 12h^2 + 4f^2] . \quad (4.7)$$

For very slow motion ($\tau \rightarrow 0$) the liquid moment should approach these values. Equation (4.5) shows that the limiting value of C_{LIM} as $\tau \rightarrow 0$ equals $(\epsilon + i)/2$. This agrees with the frozen liquid results when $\tau = 0$. When $C_r \rightarrow \infty$ the liquid should act like a frozen liquid for all values of τ . It is easy to see that the liquid moment coefficients given by Equation (4.5) approach (in the limit of $C_r \rightarrow \infty$ for λ_k not a resonance value) the values for a frozen liquid. The same limits, Equations (4.6 - 4.7), are also found when C_r and τ are arbitrary but N becomes infinitely large.

V. SOLUTION METHOD

The equations of sections III and IV need to be solved over a wide range of τ for specific values of D_ρ , f , and N . This requires calculating the ratio $J_0(\lambda_k)/J_1(\lambda_k)$ of the zero and first order Bessel functions. For values of k such that $|\lambda_k| \leq 50$, the above ratio is obtained by simply dividing the values found from power series expansions of each Bessel function. For larger values of $|\lambda_k|$, an asymptotic expansion of the Bessel function ratio was used.¹¹ Equation (4.5) is then used to find values of C_{LSM} and C_{LIM} . Experience has shown that $k < 20$ is sufficient to produce converged solutions. All computations were carried out on a VAX-8600 computer.

VI. DISCUSSION

Figures 2 and 3 present plots of C_{LSM} and C_{LIM} as functions of frequency for $f = 1.5$, $C_r = 3.0$, $N = 1$, and $\epsilon = 0$ and 0.02 . For zero damping, the maximum side moment is slightly larger than the maximum side moment for a small amount of undamping given by $\epsilon = 0.02$. The in-plane moment remains relatively unchanged due to the presence of the same undamping. This indicates that C_{LM} is insensitive to ϵ for ϵ near zero.

It was mentioned earlier that C_{LSM} and C_{LIM} approach the limiting values for a frozen liquid, Eqs. (4.6-4.7), as $C_r \rightarrow 0$. An example of this for $f = 2$, $N = 1$ and $\epsilon = 0$ is exhibited in Figures 4 and 5. Similar results are shown in Figures 6 and 7 for an increasing number of chambers N and a fixed $C_r = 3$.

Generally, it has been found that the frozen liquid limit is approached quite rapidly with increasing values of N for typical values of C_r .

If τ_0 is a Stewartson eigenfrequency for the particular values f_0 , k_0 , and N_0 , then a resonant condition will occur at $\tau = \tau_0$ whenever

$$\frac{f}{k N} = \frac{f_0}{k_0 N_0} \quad \begin{array}{l} k_0, k = 1, 3, 5, \dots \\ N_0, N = 1, 2, 3, \dots \end{array} \quad (6.1)$$

For an example of this phenomenon, consider the case of $k_0 = 1$, $f_0 = 2$, $N_0 = 1$, $C_r = 3$, and $\epsilon = 0$. These parameter values make the ratio of Equation (6.1) equal to 2 and the first eigenfrequency $\tau_0 = 0.5102$. Figure 8 shows C_{LSM} as a function of τ for $k = 1$, $f = 10$, and $N = 1, 5, 10$. The increase in C_{LSM} for $N = 5$ is due to the eigenfrequency $\tau_0 = 0.5102$ since the ratio in Eq. (6.1) is again equal to 2. Hence for a fixed τ , an increase in N can cause C_{LSM} to increase. The eigenvalues for the $N = 1, 10$ cases lie outside the range of τ given in Figure 8. C_{LSM} therefore decreases monotonically to the frozen liquid value, which is zero for $\epsilon = 0$, when N becomes sufficiently large.

The 155mm M825 projectile is shown in Figure 9. This projectile carries a canister that is loaded with white phosphorous (WP) impregnated felt wedges. Four angular ribs produce longitudinal quadrants within which felt wedges (116 per canister) are loaded. Aluminum foil spacers are located between each wedge (as shown in Figure 9) and could produce a compartmentalization or segmentation as modeled in this theory. When the WP is liquid (temperatures above 44 deg C), flight instabilities have been recorded. Recent flight tests have shown that the flight stability of the projectile can be improved by using felt wedges with outer diameters that produce interference fits when loaded into the canister.¹² The model given in this report is directed at a fundamental understanding of the payloads used in the M825. The inclusion of a drag force on the liquid caused by the permeable media provides a first step in understanding the physics of these payloads.

Scheidegger¹³ tabulated permeabilities of various substances and stated a range for hair felt as $8.3 \times 10^{-6} \text{ cm}^2 < \kappa < 1.2 \times 10^{-5} \text{ cm}^2$. For an M825-type payload, nominal values for spin rate and kinematic viscosity are 100 Hz and $0.015 \text{ cm}^2/\text{sec}$. Hence, a median drag coefficient, C_r , is $2\pi/15$ or approximately $1/2$. Experiments should be conducted to determine the permeability, κ , for the type of felt and packing used in the M825 projectile. Investigations must be conducted to verify if a linear, homogeneous formulation, using Darcy's Law, is appropriate for spinning liquids. The present analysis extends prior theories for liquid payloads and produces a simple model from which a clear physical understanding is obtained. Additions to the present effort could include the effects of fluid interaction with solid boundaries, radial variations in C_r and the nonisotropic character of C_r .

VII. CONCLUSIONS

The liquid moment coefficients are computed for cylindrical cavities which are fully-filled with a permeable medium and impregnated with an inviscid liquid. These coefficients reflect the results of segmenting a given cavity into N chambers with uniform height. The coefficients are then calculated as functions of coning frequency, fineness ratio, and the parameter C_r used to represent the physics of a liquid flowing through the permeable medium.

If the range of coning frequencies does not contain any eigenfrequencies, then the calculations plus theory indicate that the side moment approaches the value for a frozen liquid as $C_r \rightarrow 0$ and/or N becomes large. However, a significant increase in the side moment can occur for a particular N by choosing the fineness ratio such that an eigenfrequency moves into the frequency range of interest.

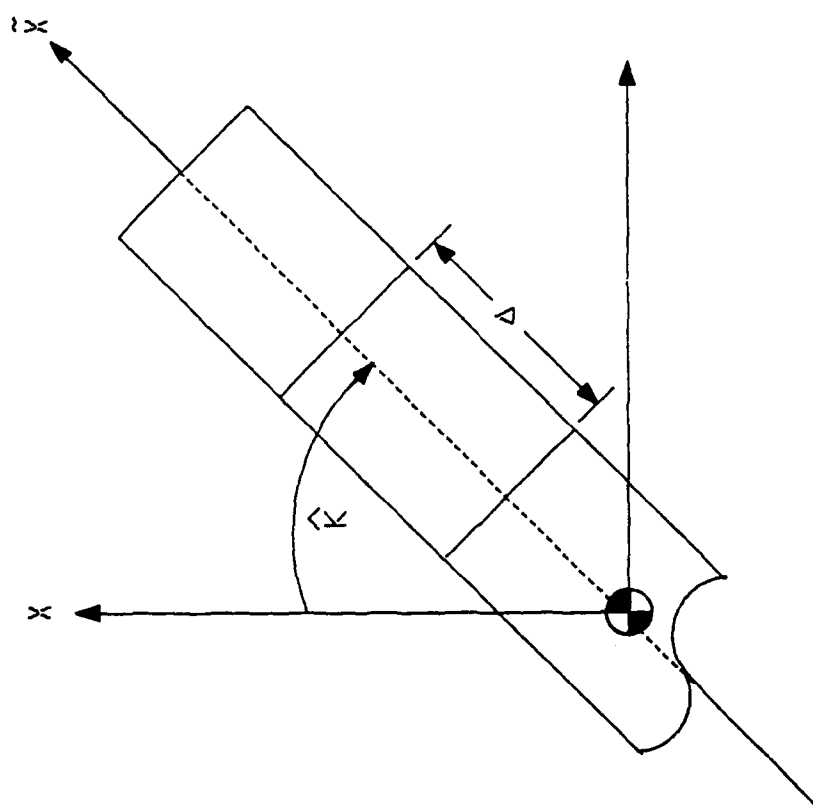


Figure 1. Diagram showing a typical cylindrical segment with impenetrable endcaps.

Aspect Ratio (c/a) = 1.5
 $C_r = 1/3, N = 1$

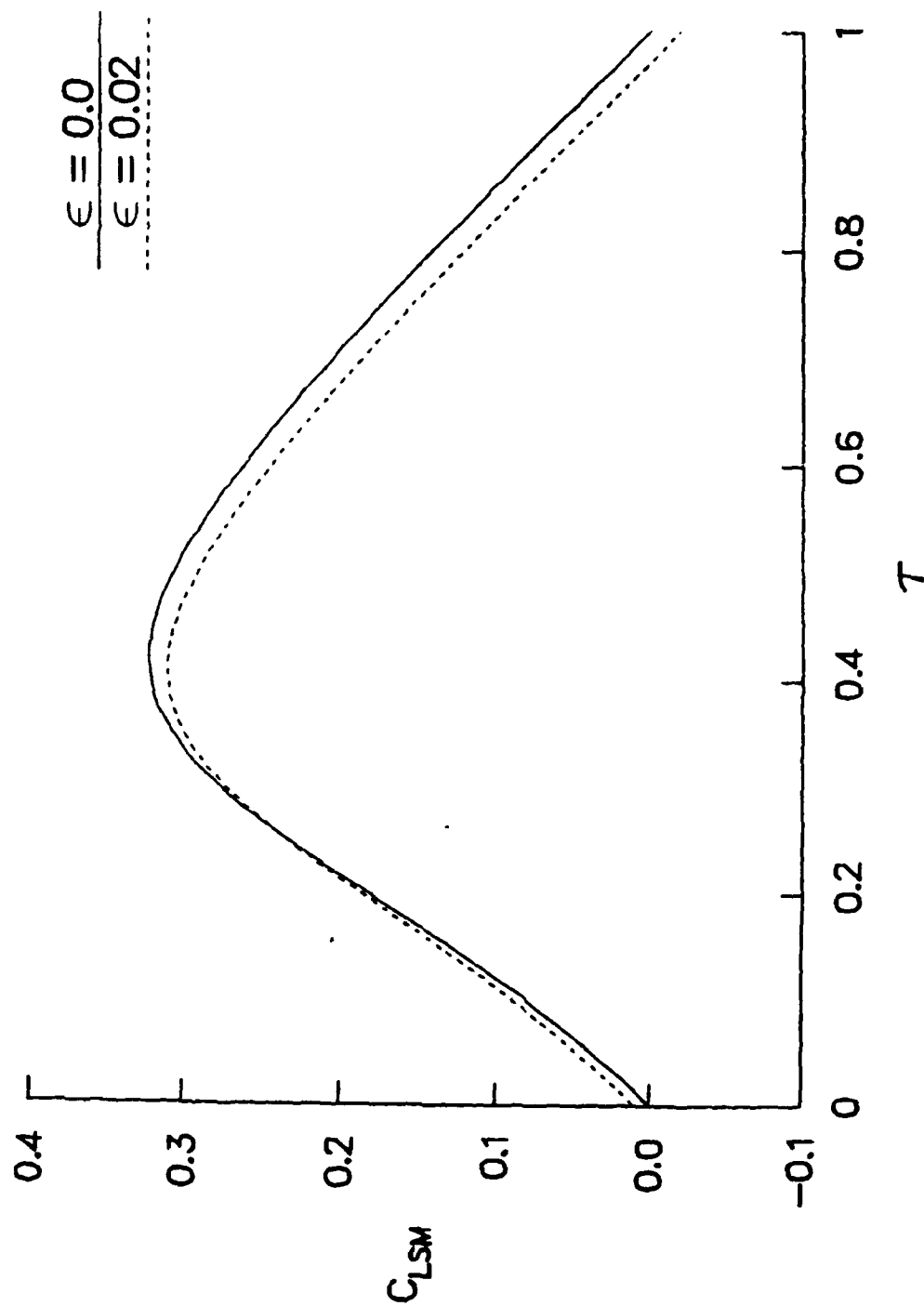


Figure 2. C_{LSM} versus τ for $f = 1.5, C_r = 3, \epsilon = 0.0, 0.02$.

Aspect Ratio (c/a) = 1.5
 $C_r = 1/3, N = 1$

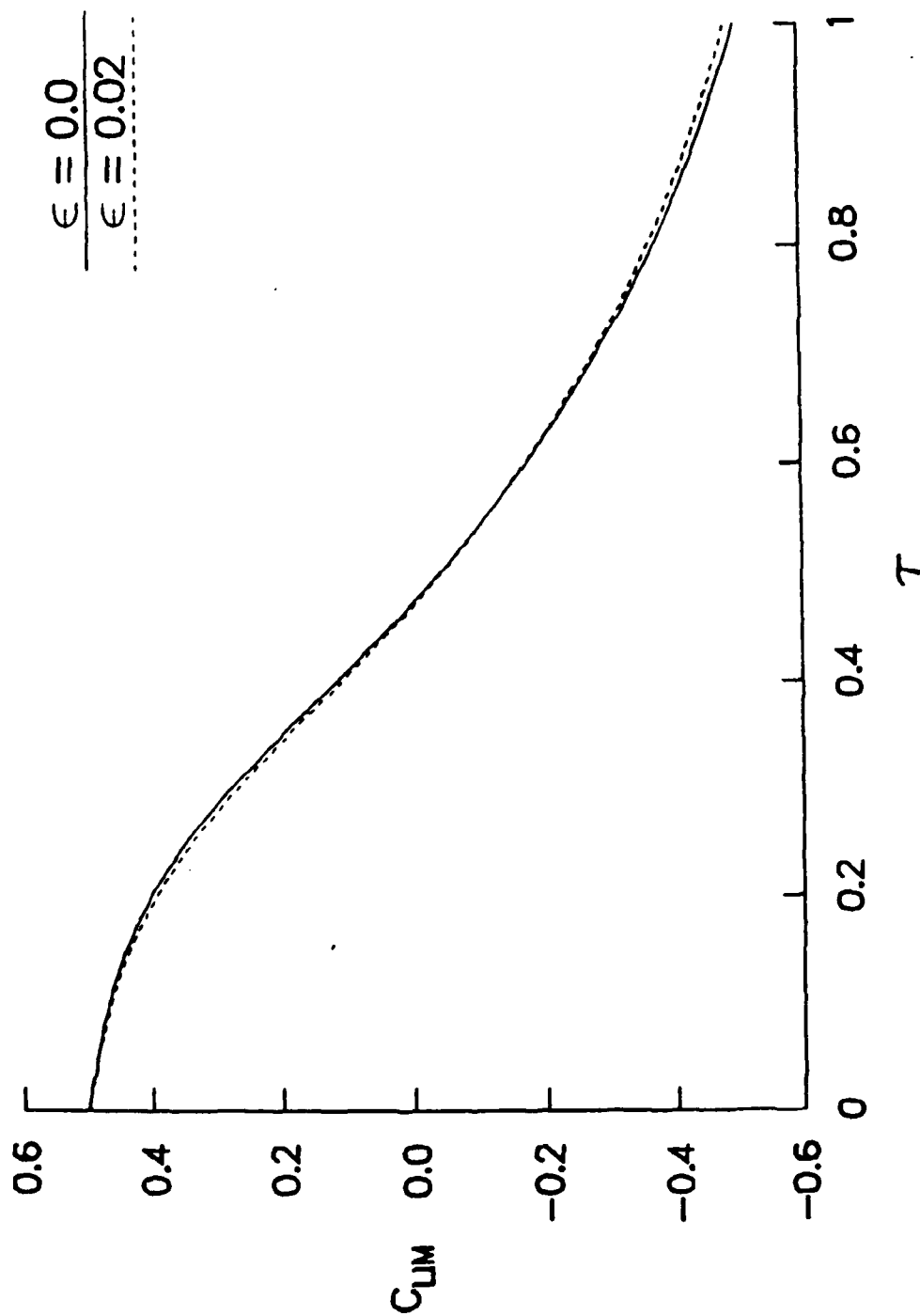


Figure 3. C_{LIM} versus τ for $f = 1.5, C_r = 3, \epsilon = 0.0, 0.02$.

Aspect Ratio (c/a) = 2.00

$N = 1, \epsilon = 0.0$

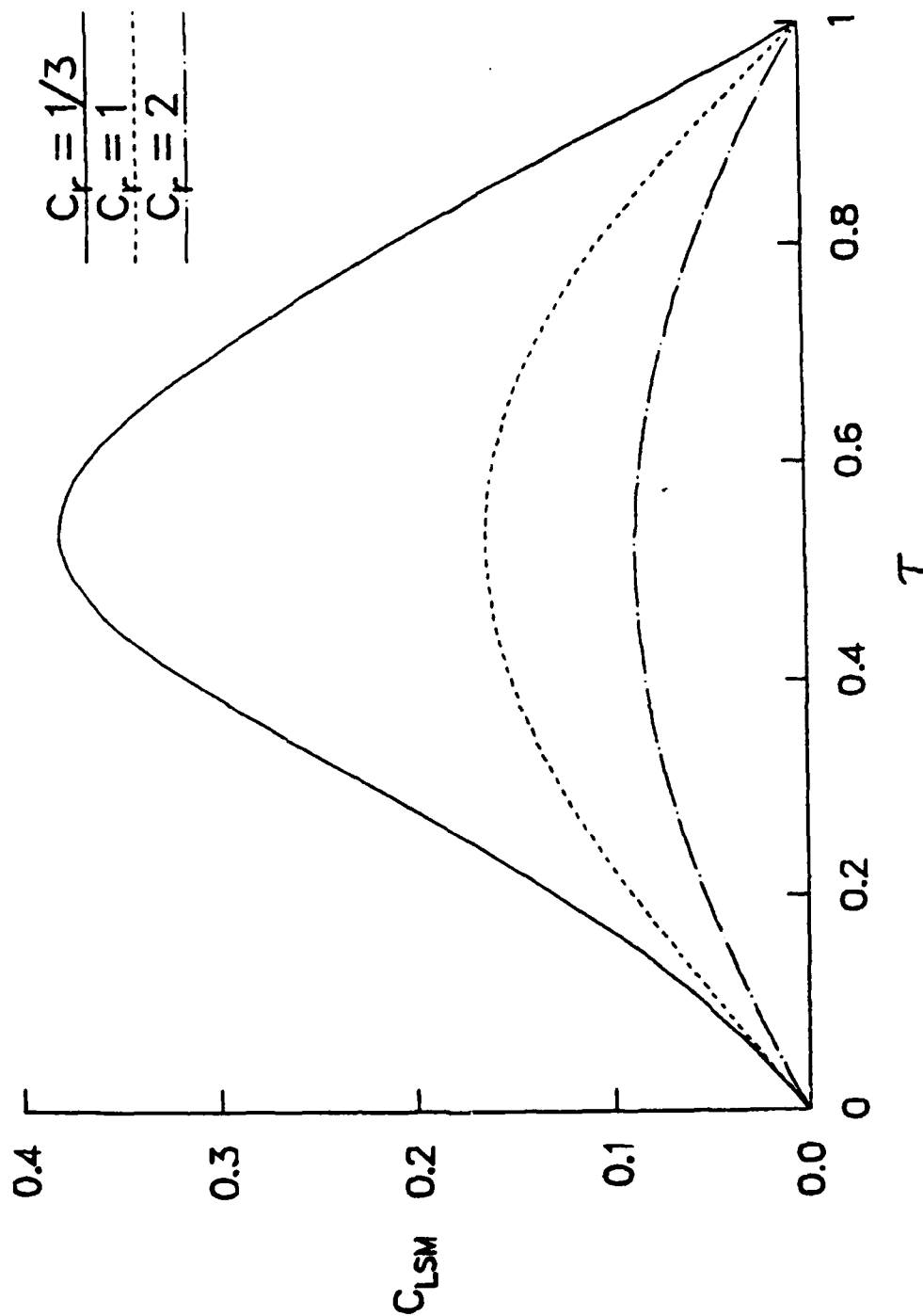


Figure 4. Comparison of C_{LSM} versus τ for $f = 2, N = 1, \epsilon = 0, C_r = 3, 1, 0.5$.

Aspect Ratio (c/a) = 2.00

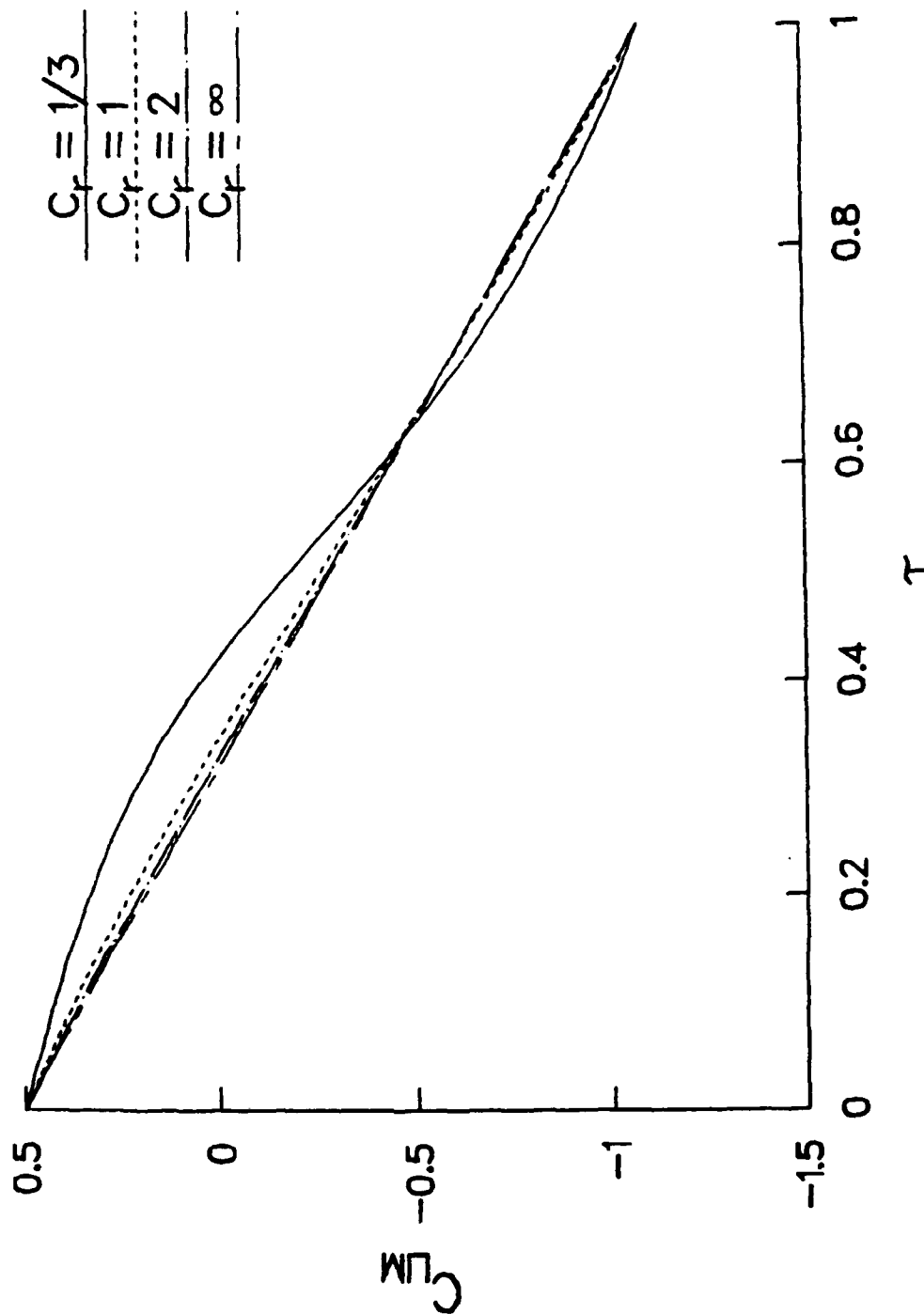


Figure 5. Comparison of C_{LIM} versus τ for $f = 1$, $N = 1$, $\epsilon = 0$, $C_r = 3, 1, 0.5$.

Aspect Ratio (c/a) = 3.00
 $C_r = 1/3, \epsilon = 0.0$

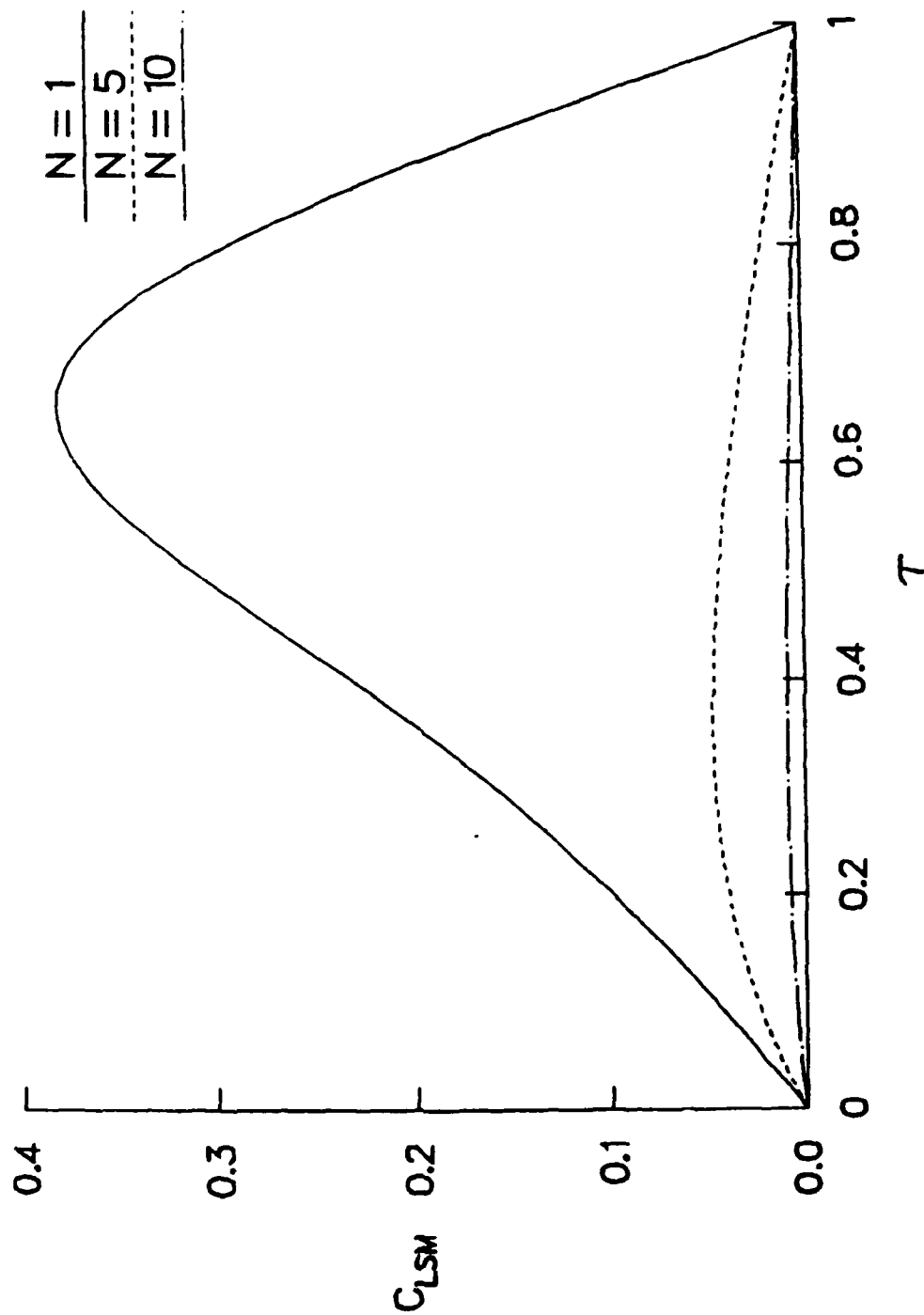


Figure 6. Comparison of C_{LSM} versus τ for $f = 3, C_r = 3, \epsilon = 0, N = 1, 5, 10$ and C_{LSM} frozen.

Aspect Ratio (c/a) = 3.00

$C_r = 1/3, \epsilon = 0.0$

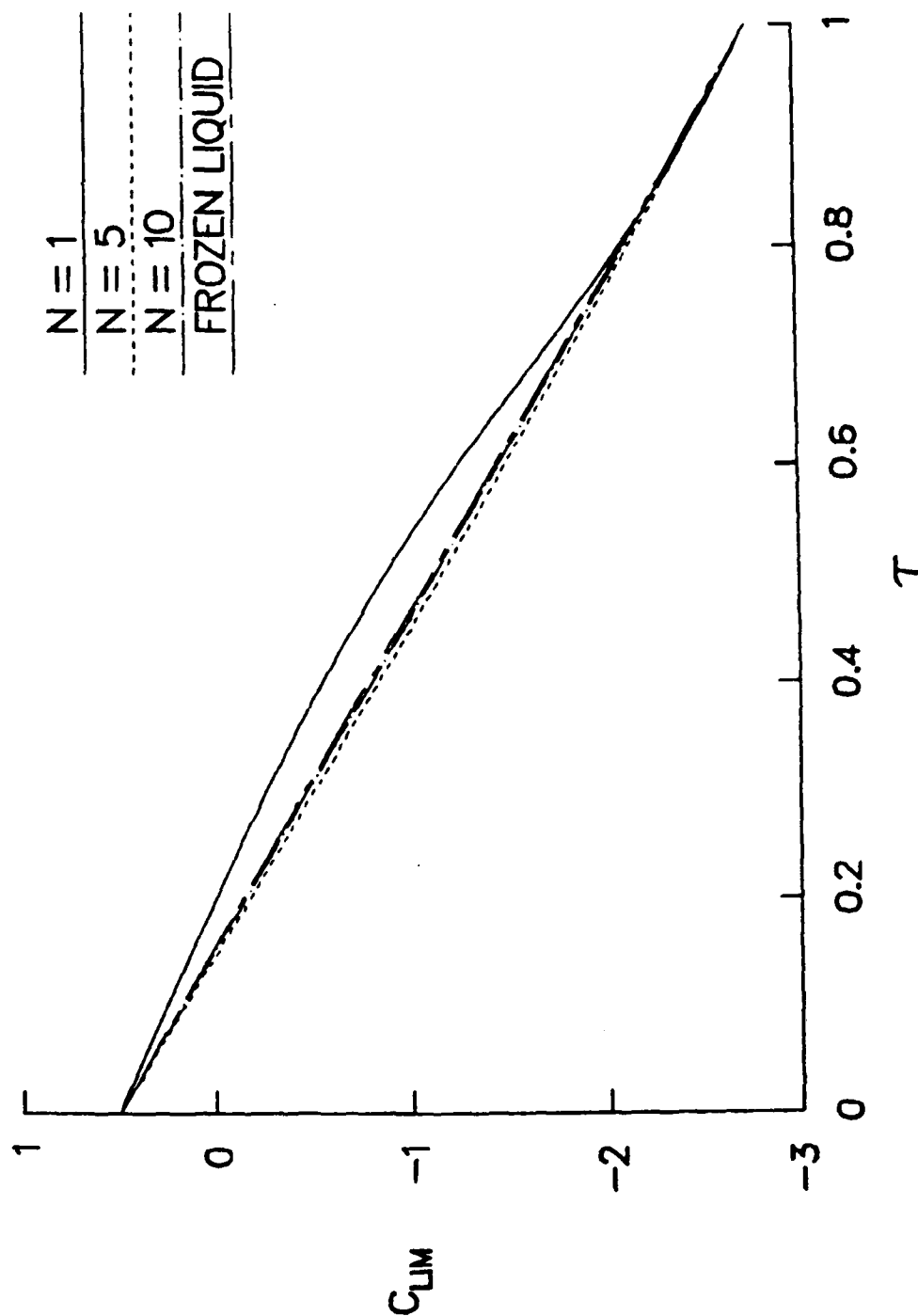


Figure 7. Comparison of C_{LIM} versus τ for $f = 3, C_r = 3, \epsilon = 0, N = 1, 5, 10$ and C_{LIM} frozen.

Aspect Ratio (c/a) = 10.0

$C_r = 1/3, \epsilon = 0.0$

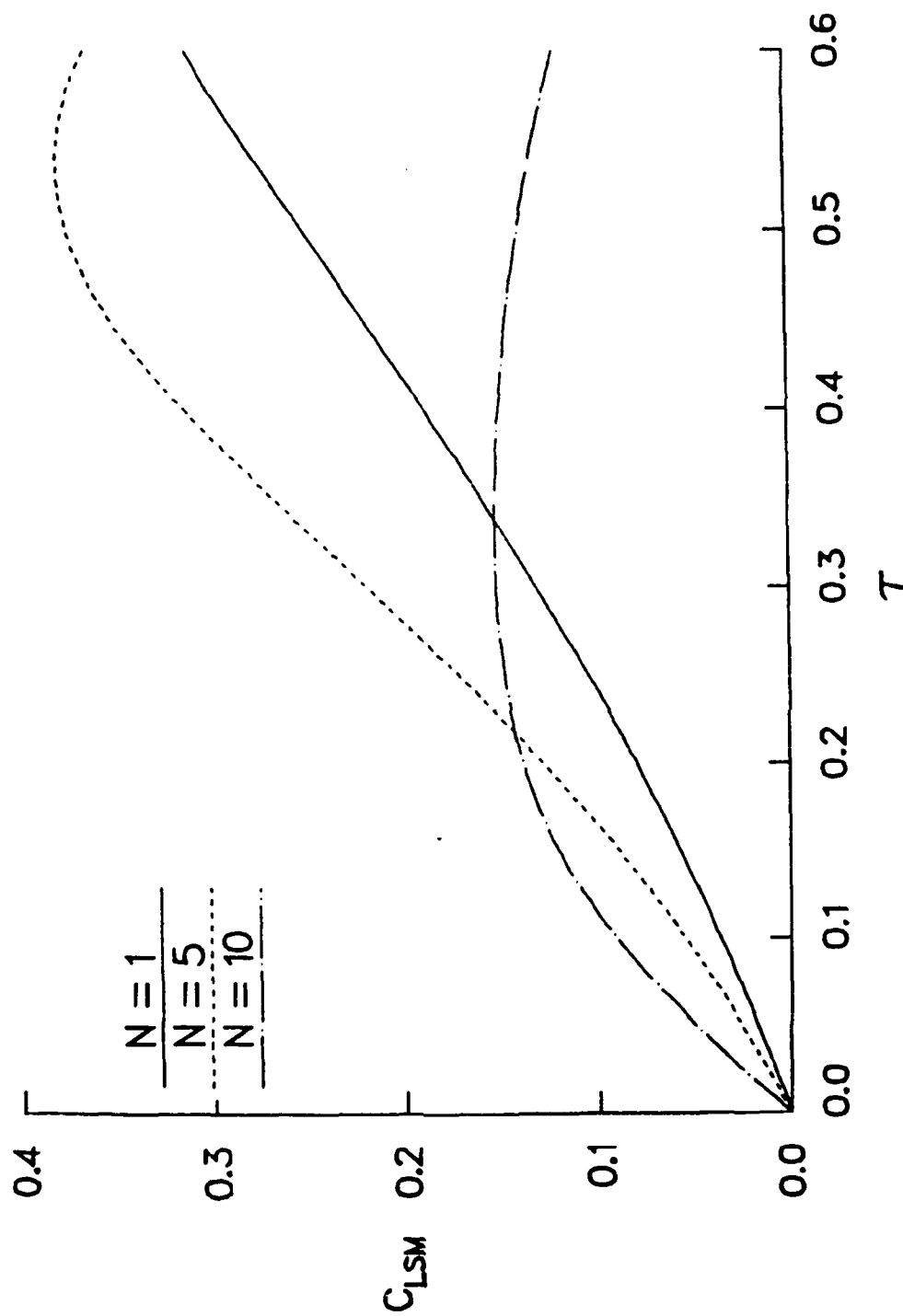


Figure 8. Comparison of C_{LSM} versus τ for $f = 10, C_r = 3, \epsilon = 0.0, N = 1, 5, 10$.

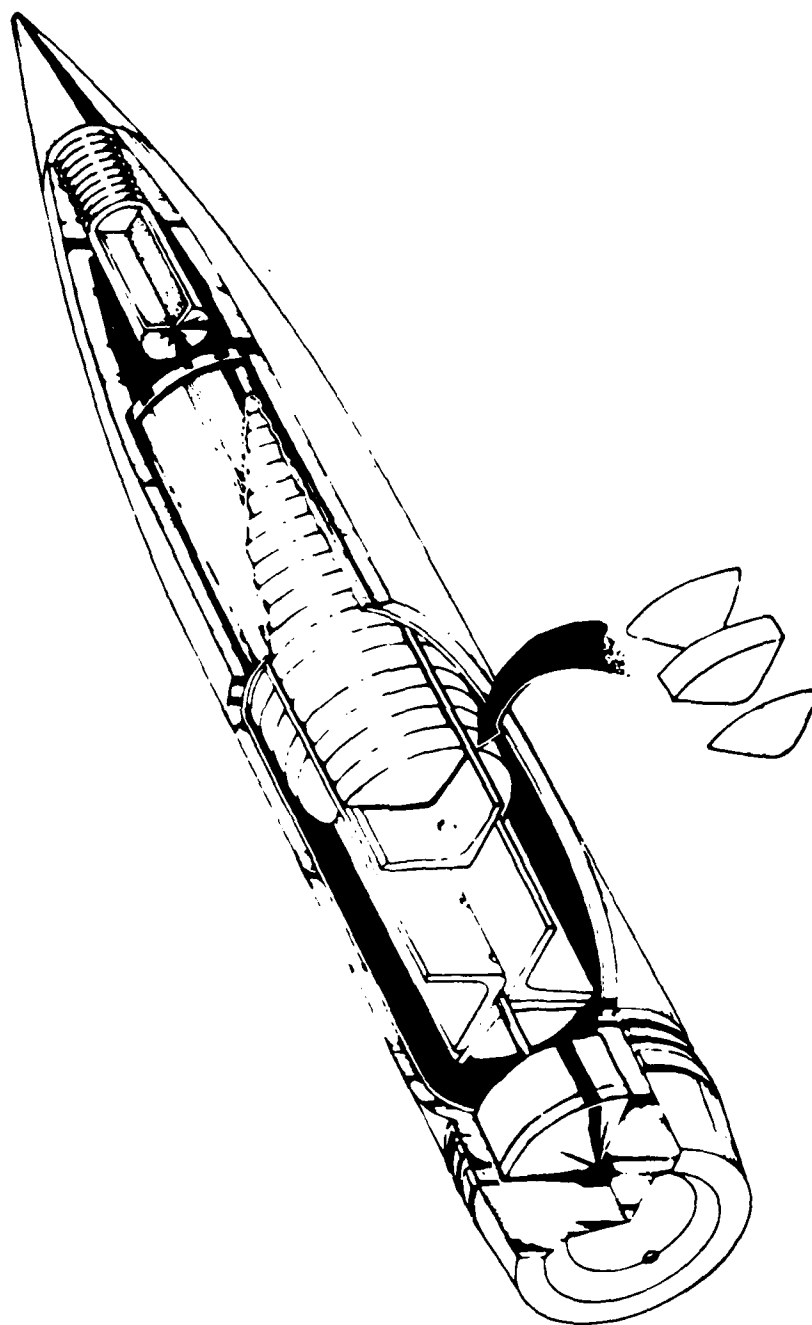


Figure 9. M825 improved smoke projectile.

REFERENCES

1. Stewartson, K., "On the Stability of a Spinning Top Containing Liquid," Journal of Fluid Mechanics, Vol. 5, Part 4, pp. 577-592, September 1959.
2. Wedemeyer, E.H., "Viscous Correction to Stewartson's Stability Criterion," BRL Report 1325, US Army Ballistic Research Laboratory, Aberdeen Proving Ground, Maryland, June 1966. (AD 489687)
3. Murphy, C.H., "Angular Motion of a Spinning Projectile with a Viscous Liquid Payload," ARBRL-MR-03194, US Army Ballistic Research Laboratory, Aberdeen Proving Ground, Maryland, August 1982. (AD A118676) (See also Journal of Guidance, Control, and Dynamics, Vol. 6, pp. 280-286, July-August 1983.)
4. Gerber, N., Sedney, R., "Moment on a Liquid-Filled Spinning and Nutating Projectile: Solid Body Rotation," ARBRL-TR-02470, US Army Ballistic Research Laboratory, Aberdeen Proving Ground, Maryland, February 1983. (AD A125332)
5. Hall, Philip, Sedney, Raymond, and Gerber, Nathan, "Fluid Motion in a Spinning, Coning Cylinder via Spatial Eigenfunction Expansions," BRL Technical Report in preparation.
6. D'Amico, W.P., and Mark, A., "The Application of a Highly Permeable Medium to Reduce Spin-Up Time and to Stabilize a Liquid-Filled Shell," ARBRL-MR-02851, US Army Ballistic Research Laboratory, Aberdeen Proving Ground, Maryland, July 1978. (AD A058595)
7. D'Amico, W.P., and Clay, W.H., "Flight Tests for Prototype Felt Wedge/White Phosphorous Improved Smoke Concept," ARBRL-MR-02824, US Army Ballistic Research Laboratory, Aberdeen Proving Ground, Maryland, April 1978. (AD A054643)
8. Morse, P. and Feshbach, H., Methods of Theoretical Physics, Vol. I, McGraw-Hill, New York, NY, 1951.
9. Darcy, H., "Les Fontaines Publiques de la Ville de Dijon," 1856.
10. Aris, R., Vectors, Tensors, and the Basic Equations of Fluid Mechanics, Prentice-Hall, Englewood Cliffs, NJ, 1962.
11. McLachlan, N.W., Bessel Functions for Engineers, Oxford University Press, London, 1955.
12. D'Amico, William P. and Soencksen, Keith P., "Aeroballistic Testing of the M825 Projectile: Phase VII - Larger Radius Felt Wedge Payloads," ARBRL-MR-3587, US Ballistic Research Laboratory, Aberdeen Proving Ground, Maryland, April 1987.
13. Scheidegger, A.E., The Physics of Flow Through Porous Media, University of Toronto Press, Canada, 1960.

LIST OF SYMBOLS

a	Maximum radial distance of the liquid-filled container (for a cylinder, the radius, for a spheroid, the radial semi-axis)
C_{LIMj}	Imaginary part of C_{LMj} ; coefficient representing the liquid moment that causes rotation in the plane of $\exp i\phi_j$, $j = 1,2$
C_{LSMj}	Real part of C_{LMj} ; coefficient representing the liquid moment that causes rotation out of the plane of $\exp (i\phi_j)$, $j = 1,2$
C_r	Drag coefficient
D_r	Drag term due porous media
$\vec{e}_x, \vec{e}_r, \vec{e}_\theta$	Unit vectors along the earth-fixed cylindrical axes
$\vec{e}_x, \vec{e}_y, \vec{e}_z$	Unit vectors along the earth-fixed Cartesian axes
f	Fineness ratio, c/a , for a cylinder
h	Distance of center of gravity along symmetry axis from geometric center
k	Axial wave number
\hat{K}	$K_{j0} e^{i\phi_{j0}}$ ($j = 1,2$)
K_j	$K_{j0} e^{\epsilon_j \tau_j \phi}$ ($j = 1,2$)
K_{j0}	Value of K_j at $t = 0$
m_L	Mass of the liquid in the container $2\pi a^2 c \rho_L$ for a cylinder; $4\pi a^2 c \rho_L / 3$ for a spheroid)
$M_{L\tilde{Y}} + M_{L\tilde{Z}}$	Transverse liquid moment in the aeroballistic nonrolling system
N	Number of products in the X factor, Eq. (3.19)
n_{XE}, n_{YE}, n_{ZE}	Earth-fixed components of a unit vector along the x-axis
p	Non-dimensional pressure perturbation as a function of r and x
r	Radial coordinate in the earth-fixed cylindrical (x,r,θ) system
$R\{\}$	Real part of $\{\}$

s	$(\epsilon_j + i)\tau_j \quad j = 1 \text{ or } 2$
u, v, w	Non-dimensional velocity perturbation components in the earth-fixed cylindrical (x, r, θ) system
\vec{V}	Non-dimensional liquid velocity perturbation, Eq. (A.3)
V_x, V_r, V_θ	Components of \vec{V} in the earth-fixed cylindrical (x, r, θ) system
x	Axial coordinate in the earth-fixed cylindrical (x, r, θ) system
XYZ	Missile-fixed axes, the X -axis along the projectile's axis of symmetry
$\tilde{X}\tilde{Y}\tilde{Z}$	Aeroballistic non-rolling axes, the \tilde{Z} -axis initially downward
$X_e Y_e Z_e$	Earth-fixed axes, the X_e -axis along the velocity vector, Z_e downward
ϵ_j	$(K_j/K_j)/\dot{\phi}_j$, non-dimensionalized damping; $j = 1, 2$
θ	Azimuthal coordinate in the earth-fixed cylindrical (x, r, θ) system
ν	Kinematic viscosity of the liquid
$\tilde{\xi}$	$\hat{K}_e s \theta$
λ_k	Defined in Eq. (3.27)
ρ_L	Liquid density
τ_j	$\dot{\phi}_j/\dot{\phi}$, non-dimensionalized frequency; $j = 1, 2$
$\dot{\phi}$	Spin rate with respect to inertial axis, assumed positive

DISTRIBUTION LIST

<u>No.</u> <u>Copies</u>	<u>Organization</u>	<u>No.</u> <u>Copies</u>	<u>Organization</u>
12	Administrator Defense Technical Information Center ATTN: DTIC-FDAC Cameron Station, Bldg. 5 Alexandria, VA 22304-6145	1	OPM Nuclear ATTN: AMCPM-NUC COL. W. P. Farmer Dover, NJ 07801-5001
1	HQDA DAMA-ART-M Washington, DC 20310	1	AFWL/SUL Kirtland AFB, NM 87117-6008
1	Commander US Army Materiel Command ATTN: AMCDRA-ST 5001 Eisenhower Avenue Alexandria, VA 22333-0001	3	Commander U.S. Armament RD&E Center US Army AMCCOM ATTN: SMCAR-AET-A Mr. R. Kline ATTN: SMCAR-AET Mr. F. Scerbo Mr. J. Bera Picatinny Arsenal, NJ 07806-5000
1	Commander US Army ARDEC ATTN: SMCAR-TDC Picatinny Arsenal, NJ 07806-5000	1	Commander US Army Armament, Munitions and Chemical Command ATTN: AMSMC-IMP-L Rock Island, IL 61299-7300
1	Commander U.S. Armament RD&E Center US Army AMCCOM ATTN: SMCAR-MSI Picatinny Arsenal, NJ 07806-5000	1	Commander U.S. AMCCOM ARDEC CCAC Benet Weapons Laboratory ATTN: SMCAR-CCB-TL Watervliet, NY 12189-4050
1	Commander U.S. Armament RD&E Center US Army AMCCOM ATTN: SMCAR-LC Picatinny Arsenal, NJ 07806-5000	1	Commander US Army Aviation Systems Command ATTN: AMSAV-ES 4300 Goodfellow Blvd St Louis, MO 63120-1789
1	Commander U.S. Army AMCCOM ATTN: SMCAR-CAWS-AM Mr. DellaTerga Picatinny Arsenal, NJ 07806-5000		

DISTRIBUTION LIST

<u>No.</u> <u>Copies</u>	<u>Organization</u>	<u>No.</u> <u>Copies</u>	<u>Organization</u>
1	Director US Army Aviation Research and Technology Activity Moffett Field, CA 94035-1099	1	Director US Army Missile and Space Intelligence ATTN: AIAMS-YDL Redstone Arsenal, AL 35898-5500
1	Commander US Army Communications Electronics Command ATTN: AMSEL-ED Fort Monmouth, NJ 07703-5000	1	Commander US Army Tank Automotive Command ATTN: AMSTA-TSL Warren, MI 48397-5000
1	Commander CECOM R&D Technical Library ATTN: AMSEL-IM-L, (Reports Section) B. 2700 Fort Monmouth, NJ 07703-5000	1	Director US Army TRADOC Analysis Center ATTN: ATOR-TSL White Sands Missile Range NM 88002-5502
10	C. I. A. OIC/DB/Standard GE47 HQ Washington, DC 20505	1	Commander US Army Development & Employment Agency ATTN: MODE-ORO Fort Lewis, WA 98433-5000
1	Commandant US Army Infantry School ATTN: ATSH-CD-CS-OR Fort Benning, GA 31905-5400	1	Commandant US Army Field Artillery School ATTN: ATSF-GD Fort Sills, OK 73503
1	Commander US Army Missile Command Research Development and Engineering Center ATTN: AMSMI-RD Redstone Arsenal, AL 35898-5230	1	Director National Aeronautics and Space Administration Langley Research Center ATTN: Tech Library Langley Station Hampton, VA 23365
1	Commander US Army Missile Command ATTN: AMSMI-RDK, Mr. Dahlke Redstone Arsenal, AL 35898-5230	1	Director US Army Field Artillery Board ATTN: ATZR-BDW Fort Sills, OK 73503

DISTRIBUTION LIST

<u>No.</u> <u>Copies</u>	<u>Organization</u>	<u>No.</u> <u>Copies</u>	<u>Organization</u>
1	Commander US Army Dugway Proving Ground ATTN: STEDP-MT Mr. G. C. Travers Dugway, UT 84022	1	Director National Aeronautics and Space Administration Marshall Space Flight Center ATTN: Dr. W. W. Fowlis Huntsville, AL 35812
1	Commander US Army Yuma Proving Ground ATTN: STEYP-MTW Yuma, AZ 85365-9103	1	Director National Aeronautics and Space Administration Ames Research Center ATTN: Dr. J. Steger Moffet Field, CA 94035
2	Director Sandia National Laboratories ATTN: Dr. W. Oberkampff Dr. W. P. Wolfe Division 1636 Albuquerque, NM 87185	1	Calspan Corporation ATTN: W. Rae P.O. Box 400 Buffalo, NY 14225
1	Air Force Armament Laboratory ATTN: AFATL/DLODL (Tech Info Center) Eglin AFB, FL 32542-5438	2	Rockwell International ATTN: Dr. V. Shankar Dr. S. Chakravarthy 1049 Camino Dos Rios Thousand Oaks, CA 91360
1	Commander Naval Surface Weapons Center ATTN: Dr. W. Yanta Aerodynamics Branch K-24, Building 402-12 White Oak Laboratory Silver Spring, MD 20910	1	University of Santa Clara Department of Physics ATTN: R. Greeley Santa Clara, CA 95053
1	Carco Electronics 195 Constitution Drive Menlo Park, CA 94025	1	Arizona State University Department of Mechanical and Energy Systems Engineering ATTN: G.P. Neitzel Tempe, AZ 85281
1	Aerospace Corporation Aero-Engineering Subdivision ATTN: Walter F. Reddall El Segundo, CA 90245		

DISTRIBUTION LIST

<u>No.</u> <u>Copies</u>	<u>Organization</u>	<u>No.</u> <u>Copies</u>	<u>Organization</u>
1	Massachusetts Institute of Technology ATTN: H. Greenspan 77 Massachusetts Avenue Cambridge, MA 02139	2	Director Lawrence Livermore National Laboratory ATTN: Mail Code L-35 Mr. T. Morgan Mr. R. Cornell P.O. Box 808 Livermore, CA 94550
1	North Carolina State University Mechanical and Aerospace Engineering Department ATTN: F.F. DeJarnette Raleigh, NC 27607	1	University of Wisconsin-Madison Center for Mathematical Sciences ATTN: Dr. John Strikwerda 610 Walnut Street Madison, WI 53706
1	Northwestern University Department of Engineering Science and Applied Mathematics ATTN: Dr. S.H. Davis Evanston, IL 60201	1	Virginia Polytechnic Institute and State University Department of Aerospace Engineering ATTN: Tech Library Blacksburg, VA 24061
1	University of Colorado Department of Astro-Geophysics ATTN: E.R. Benton Boulder, CO 80302	2	University of Southern California Department of Aerospace Engineering ATTN: T. Maxworthy P. Weidman Los Angeles, CA 90007
2	University of Maryland ATTN: W. Melnik J.D. Anderson College Park, MD 20740	1	Hughes Aircraft ATTN: Dr. John McIntyre Mail Code S41/B323 P.O. Box 92919 Los Angeles, CA 90009
1	University of Maryland Baltimore County Department of Mathematics ATTN: Dr. Y.M. Lynn 5401 Wilkens Avenue Baltimore, MD 21228		
1	Rensselaer Polytechnic Institute Department of Math Sciences Troy, NY 12181		

DISTRIBUTION LIST

<u>No.</u> <u>Copies</u>	<u>Organization</u>	<u>No.</u> <u>Copies</u>	<u>Organization</u>
1	Ohio State University Dept. of Mechanical Engineering ATTN: Dr. T. Herbert Columbus, OH 43210		Aberdeen Proving Ground Director, USAMSAA ATTN: AMXSY-D AMXSY-RA, R. Scungio
1	Mr. Harold Vaughn 7709 Gladden N.E. Albuquerque, NM 87110		Commander, UASTECOM ATTN: AMSTE-SI-F AMSTE-TE-F, W. Vomocil PM-SMOKE, Bldg. 324
1	Illinois Institute of Technology ATTN: Mr. Simon Rosenblat 3300 South Federal Chicago, Illinois 60616		ATTN: AMCPM-SMK-M Mr. J. Callahan Cdr, CRDC, AMCCOM ATTN: SMCCR-MU Mr. W. Dee Mr. C. Hughes Mr. F. Dagostin Mr. D. Bromley Mr. C. Jeffers Mr. L. Shaft ATTN: SMCCR-RSP-A Mr. Miles Miller ATTN: SMCCR-SPS-IL SMCCR-RSP-A SMCCR-MU

USER EVALUATION SHEET/CHANGE OF ADDRESS

This Laboratory undertakes a continuing effort to improve the quality of the reports it publishes. Your comments/answers to the items/questions below will aid us in our efforts.

1. BRL Report Number _____ Date of Report _____
2. Date Report Received _____
3. Does this report satisfy a need? (Comment on purpose, related project, or other area of interest for which the report will be used.) _____

4. How specifically, is the report being used? (Information source, design data, procedure, source of ideas, etc.) _____

5. Has the information in this report led to any quantitative savings as far as man-hours or dollars saved, operating costs avoided or efficiencies achieved, etc? If so, please elaborate. _____

6. General Comments. What do you think should be changed to improve future reports? (Indicate changes to organization, technical content, format, etc.) _____

CURRENT
ADDRESS

Name

Organization

Address

City, State, Zip

7. If indicating a Change of Address or Address Correction, please provide the New or Correct Address in Block 6 above and the Old or Incorrect address below.

OLD
ADDRESS

Name

Organization

Address

City, State, Zip

(Remove this sheet, fold as indicated, staple or tape closed, and mail.)

----- FOLD HERE -----

Director
US Army Ballistic Research Laboratory
ATTN: DRXBR-OD-ST
Aberdeen Proving Ground, MD 21005-5066

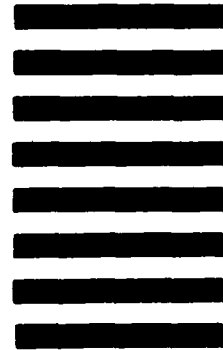


NO POSTAGE
NECESSARY
IF MAILED
IN THE
UNITED STATES

OFFICIAL BUSINESS
PENALTY FOR PRIVATE USE. \$300

BUSINESS REPLY MAIL
FIRST CLASS PERMIT NO 12062 WASHINGTON, DC
POSTAGE WILL BE PAID BY DEPARTMENT OF THE ARMY

Director
US Army Ballistic Research Laboratory
ATTN: DRXBR-OD-ST
Aberdeen Proving Ground, MD 21005-9989



----- FOLD HERE -----

END

DATE

FILMED

8-88

DTIC